Chapter 4

Application of Nuclear Magnetic Resonance Spectroscopy (NMR) to Study the Properties of Liposomes

Anna Timoszyk

Additional information is available at the end of the chapter

http://dx.doi.org/10.5772/intechopen.68522

Abstract

The liposomes are well-known lipid aggregates. The lipid composition and size of the liposomes can be controlled. The method of preparation, lipid composition, temperature, and pH have an influence on the liposome size and bilayer structure. The physicochemical properties of liposomes allow them to various applications. Nuclear magnetic resonance (NMR) is one of the methods used to study liposome properties. The abilities of the method are the high sensitivity and high resolution. Moreover, it provides information about dynamics and structure of molecules. ^{1}H and ^{31}P NMR are most convenient methods to study liposomes, because liposomes are typically formed from phospholipids. Additionally, two-dimensional NMR spectroscopy reveals information about the nature of intermolecular and intramolecular interactions (scalar and dipole-dipole interactions) that makes easier to interpret the structure of molecules. The chapter aims to introduce the NMR phenomenon, interactions between spins in magnetic field, dynamics of molecules and physical parameters of NMR spectra, and the necessary information for analyzing and interpreting high-resolution NMR spectra. It also aims to show how various changes in the bilayer structure or dynamics of lipid molecules are visible in the NMR spectra.

Keywords: liposomes, nuclear magnetic resonance, dynamics, half-width of signal, signal splitting, ^{1}H NMR, ^{31}P NMR, 2D NMR

1. Introduction

Nuclear magnetic resonance (NMR) spectroscopy provides information about the structure and dynamics at the molecular level. The knowledge about the peculiarity of NMR phenomenon and about the physical parameters of NMR spectra would help in analyzing obtained results.

1.1. The magnetic properties and magnetic moment of nuclei

Studies of the atomic structure of discrete spectra have shown that, similar to electrons, nuclei have momentum, which is called nuclear spin. Nuclear spin is directly connected to a given magnetic moment. The values of these magnetic moments can vary. The magnetic moment $\vec{\mu}$ is proportional to momentum $\vec{K}$ (spin) [1]:

$$\vec{\mu} = \gamma \vec{K} \tag{1}$$

where γ is the gyromagnetic ratio, characteristic for a given nucleus (**Table 1**)

1.2. Resonance condition

A given nucleus with its magnetic moment and spin will precess in intense static magnetic field B_0 with frequency ω_0:

$$\omega_0 = 2\pi\nu. \tag{2}$$

The value of the frequency is proportional to γ and to the B_0 field [1]:

$$\omega_0 = \gamma B_0. \tag{3}$$

The frequency of precession in the B_0 field is known as Larmor frequency. In precession, the nuclear dipoles move around a cone in the B_0 field at frequency ω_0. The precessing nuclei transverse magnetic field B_1, which is a linearly oscillating magnetic field along the x-axis, and they then submit to the combined action of both the B_0 and B_1 fields [1]. If B_1 field oscillates at the Larmor frequency, the nuclear magnetic resonance phenomenon will be observed, according to resonance condition as follows:

$$\omega_1 = \omega_0 = \gamma B_0. \tag{4}$$

Nuclei	Nuclear spin	Gyromagnetic ratio [$T^{-1}{\cdot}s^{-1}$]	Resonance frequency in $B_0 = 14.092$ T [MHz]
^{1}H	1/2	2.6752×10^{8}	600
^{13}C	1/2	6.7266×10^{7}	150.9
^{15}N	1/2	-2.7108×10^{7}	60.8
^{17}O	5/2	-3.6267×10^{8}	81.4
^{19}F	1/2	2.5167×10^{8}	564.5
^{25}Mg	5/2	-1.6371×10^{7}	36.7
^{31}P	1/2	1.0829×10^{8}	243.9
^{33}S	3/2	2.0518×10^{7}	46
^{35}Cl	3/2	2.6213×10^{7}	58.8
^{39}K	3/2	1.2482×10^{7}	28

Table 1. The values of nuclear spin ($\vec{K}$), gyromagnetic ratio (γ), and resonance frequency (ω_0) [1, 3].

1.3. Nuclear magnetic relaxation

The nuclear magnetic relaxation phenomenon is connected to the interaction between the magnetization vector $\vec{M}$ (equilibrium magnetization) and the B_0 field. The $\vec{M}$ vector is the sum of the magnetic moments of the given nuclei:

$$\vec{M} = \sum_{i=1}^{n} \vec{\mu}_i. \tag{5}$$

The value of magnetization is equal to zero when the nuclei are not in the B_0 field. Then, the $\vec{\mu}$ moments of the nuclei are oriented chaotically in accordance with statistical distribution. In the B_0 field, the $\vec{\mu}$ vectors are ordered, which results in thermodynamic equilibrium. The time in which the equilibrium is set depends on the type of sample and the temperature [2]. In the equilibrium state, more $\vec{\mu}$ moments are oriented parallel to the B_0 field than are antiparallel to it. It is in agreement with the normal Boltzmann equilibrium between the spin states. Thus, the $\vec{M}$ vector is also oriented along the direction of the B_0 field (**Figure 1**).

The $\vec{\mu}$ moments are not coherent in precession; thus, there is no gain in the transverse magnetization $\overrightarrow{M_{xy}}$. When the B_1 field interacts with the precessing spins at the Larmor frequency, the $\overrightarrow{M_{xy}}$ vector gains (**Figure 2**) [2].

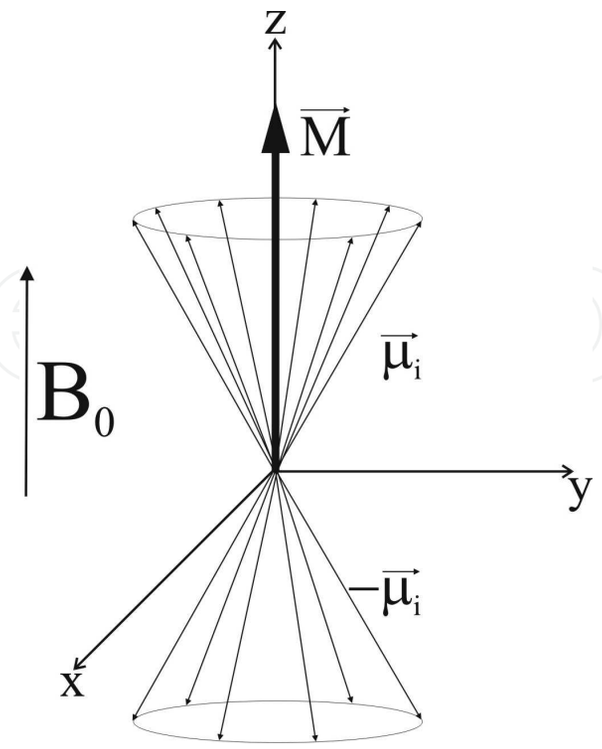

Figure 1. Equilibrium magnetization $\vec{M}$ in B_0 field.

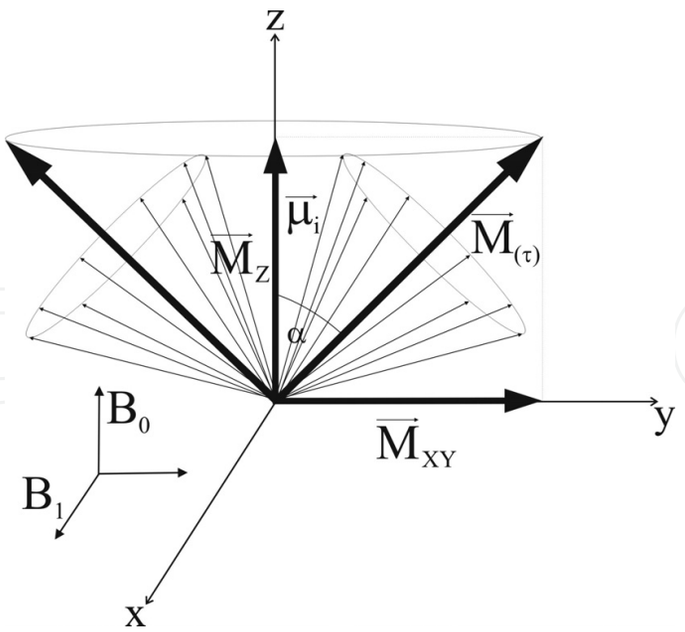

Figure 2. The $\vec{M}$ vector emerged at angle α with respect to the z-axis and the transverse $\vec{M}_{xy}$.

After switching off the B_1 field at time τ, the $\vec{M}$ vector will emerge at angle $\alpha = \gamma B_1 \tau$ with respect to the z-axis. Then, the $\vec{M}$ vector begins to precess around the direction of B_0 field, which is now active [1]. Thus, the transverse $\vec{M}_{xy}$ will lose at time T_2 (transverse relaxation time or spin-spin relaxation time) (**Figure 3**).

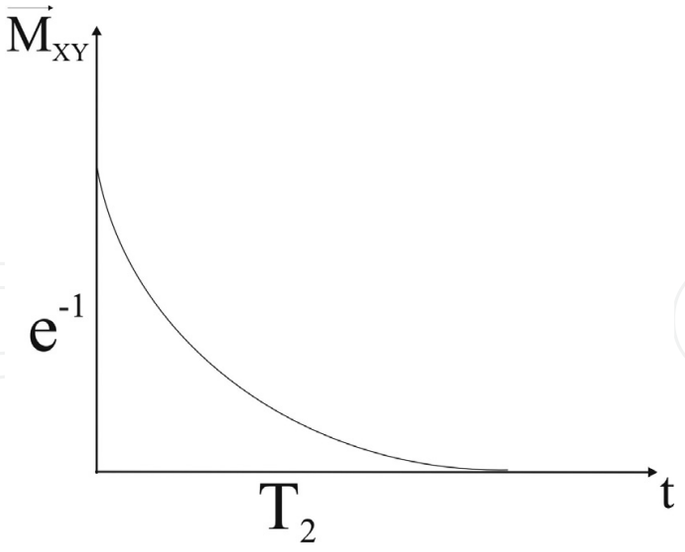

Figure 3. The loss of transverse $\vec{M}_{xy}$ vector at time T_2.

1.3.1. Spin-lattice relaxation process

The orientation of the $\vec{\mu}$ in magnetic field B_0 depends on the value of the interaction energy between $\vec{\mu}$ and B_0 field [3]:

$$E = -\vec{\mu}\, B_0 = -m\gamma B_0, \tag{6}$$

where m is the magnetic quantum number.

In the equilibrium, the nuclei at every energetic level are in accordance with the normal Boltzmann equilibrium law [3]:

$$\frac{N_1}{N_2} = \exp\frac{\Delta E}{RT} \approx 1 + \frac{\gamma\hbar B_0}{kT_L}, \tag{7}$$

where N_1 is the nucleus population on the energy state, which is less than ΔE energy in comparison to the N_2 population, T_L is the sample temperature, and $\hbar = h/2\pi$ where h is Planck constant.

The B_1 field induces the transition between quantum states, which gives rise to the NMR signal. The equalization of Boltzmann populations (extinction of NMR signal) in the quantum states, known as saturation phenomenon, is accompanied by an increase in the spin temperature T_S. At the same moment, the sample temperature T_L does not change. The condition in which $T_\mathrm{S} > T_\mathrm{L}$means that the equilibrium state has not been archived; however, after switching off the B_1 field, the T_S temperature will equalize with T_L (lattice) temperature. The spin existing in the excited quantum state cannot return to the ground state spontaneously. Thus, forced emission is one way that the spins lose energy [4]. This type of emission is possible only throughout spin-lattice interactions. The transitions between the spin states can be enforced only via the local magnetic field B_loc at the Larmor frequency. Fluctuations of B_loc field are generated by the thermal motion of the atoms and molecules from which a network is formed [1, 2]. Each magnetic moment that participates in random rotational or translational Brownian motion causes a fluctuation of the B_loc field, which causes a Fourier's frequency spectrum for those fields. For the spin ½ nuclei ^{1}H, ^{13}C, and ^{31}P, the dominant mechanism of relaxation is a dipole-dipole interaction, which is a result of the interaction between $\vec{\mu}$ and B_loc that is generated by neighboring magnetic moments. Thus, for the spin ½ nuclei, the dominant mechanism of relaxation is the interaction between the gradient of the electric field generated at the location of the observed nucleus by its electrical surroundings and nuclear electric quadrupole moment [4–6].

The simplest way to describe dipole-dipole interaction is by using the system of two spins. If the spin $I\left(\vec{\mu_I}\right)$ is near the second spin $S\left(\vec{\mu_S}\right)$, then the B_loc field created by the nucleus S at the position of nucleus I is equal to [1–3]

$$B_\mathrm{loc} = \pm\frac{\vec{\mu_S}}{\vec{R_\mathrm{IS}}}\left(3\cos^2\theta - 1\right), \tag{8}$$

where θ is the angle between the B_0 field and the $\vec{R_{IS}}$ vector, and $\vec{R_{IS}}$ vector is the distance between spin I and spin S (**Figure 4**).

If spins S and I are from the same molecule, then the $\vec{R_{IS}}$ is constant, and fluctuations in the B_loc will be associated with random changes in the angle. This mechanism of relaxation is known

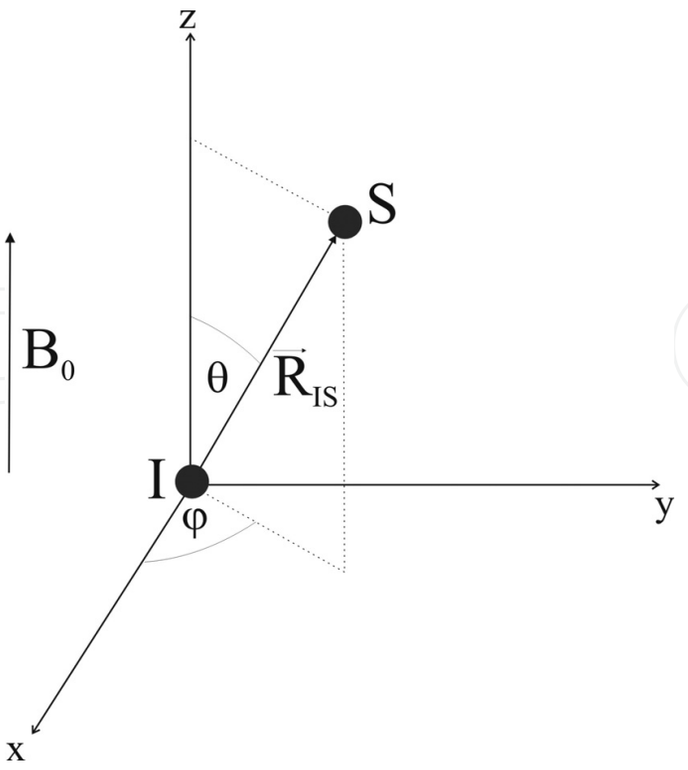

Figure 4. The system of two spins in magnetic field.

as rotational or intermolecular relaxation. If spin I and spin S are not from the same molecule, then the B_{loc} field fluctuations will depend on changes in both angle and the length of the $\vec{R_{IS}}$ [2]. This is called as translational or intramolecular mechanism of relaxation, which primarily relates to a liquid. In fact, in the spin I position, the B_{loc} field is produced by more than one spin S; however, if a system has more than two spins, the calculation of relaxation time rate is limited and the additivity of the effects is assumed. Then, the rate of the spin-lattice relaxation time T_1 can be expressed as the sum of the probabilities of the transitions between spin energy levels [6]:

$$\frac{1}{T_1} = \frac{\sum_{MM'} W_{MM'}(E_M - E_{M'})^2}{\sum_M E_M^2}, \tag{9}$$

where $W_{MM'}$ is the probability of the transition between energy level E_M and level $E_{M'}$.

In the case in which the two protons will be taken into consideration, for example, in an H_2O molecule, then the rate of T_1 can be summarized as follows [2]:

$$\frac{1}{T_1} = 2(W_1 + W_2), \tag{10}$$

where w_1 is the probability of a single spin-flip transition, and w_2 is the probability of a double spin-flip transition.

In a system of AX spins, for example, in a CH group, the cross-relaxation effect occurs. In such a case, it is necessary to use the proton-decoupling method to prevent the splitting of signals (multiplets) caused by the spin-spin couplings. Then, the rate of T_1 can be expressed by the formula [2]:

$$\frac{1}{T_1} = W_0 + 2W_1 + W_2, \tag{11}$$

where w_0, w_1, and w_2 represent the probabilities of the two-spin system (**Figure 5**).

After determining the transition probabilities and the perturbation Hamiltonian, it is possible to write the T_1 relaxation time for the homonuclear spins (II) and heteronuclear spins (IS) as follows [5]:

$$\frac{1}{T_1} = \frac{3}{10}\gamma_I^4\hbar^2 R_{II}^{-6}\left[\frac{\tau_c}{1+\omega_I^2\tau_c^2} + \frac{4\tau_c}{1+4\omega_I^2\tau_c^2}\right] \tag{12}$$

and

$$\frac{1}{T_1} = \frac{1}{10}\gamma_I^2\gamma_S^2\hbar^2 R_{IS}^{-6}\left[\frac{\tau_c}{1+(\omega_S-\omega_I)^2\tau_c^2} + \frac{3\tau_c}{1+\omega_I^2\tau_c^2} + \frac{6\tau_c}{1+(\omega_S+\omega_I)^2\tau_c^2}\right], \tag{13}$$

where τ_c is the correlation time.

The time T_1 is very sensitive to the length of $\vec{R_{IS}}$ between near spins, as directly proportional to its sixth power [7].

The high-temperature approximation is fulfilled, $\omega_0^2\tau_c^2 \ll 1$, for liquids, thus the rate of T_1 is independent of the frequency and Eqs. (12) and (13) are simplified to the following forms [2]:

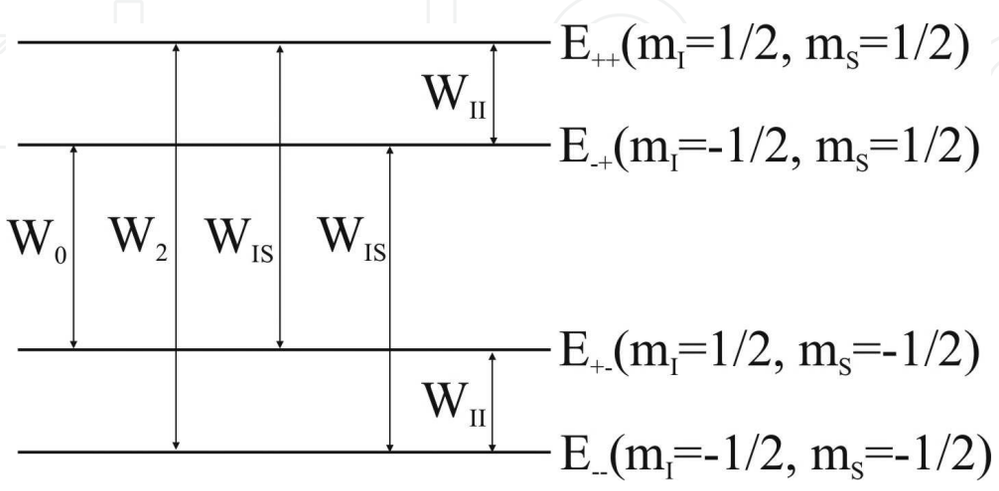

Figure 5. The unlimited transitions in two spin system.

$$\frac{1}{T_1} = \frac{3}{2}\frac{\gamma_I^4 \hbar^2}{\vec{R}_{II}^6}\tau_c \tag{14}$$

and

$$\frac{1}{T_1} = \frac{3}{2}\frac{\gamma_I^2 \gamma_S^2 \hbar^2}{\vec{R}_{II}^6}\tau_c. \tag{15}$$

As a result of the high-temperature approximation, the rate of T_1 increases as the temperature increases.

In general, the total rate of T_1 for protons is the sum of the rates of relaxation times caused by intermolecular and intramolecular factors [2]:

$$\frac{1}{T_1} = \left(\frac{1}{T_1}\right)_{\text{intra}} + \left(\frac{1}{T_1}\right)_{\text{inter}}, \tag{16}$$

where the rate of relaxation time, denoted as intramolecular $(1/T_1)_{\text{intra}}$, fulfills relation (14).

The calculation of the rate of relaxation time caused by the intermolecular factors was presented in reference [8]. The $(1/T_1)_{\text{inter}}$ is directly proportional to the population of spins N_1, and it is inversely proportional to the translational diffusion coefficient D:

$$\left(\frac{1}{T_1}\right)_{\text{inter}} = \frac{17}{30}\frac{\pi\gamma_I^4 \hbar N_1}{aD}, \tag{17}$$

where a is the closest possible distance between two spins belonging to two molecules (a is usually equal to the particle diameter).

Thus, D can be obtained directly while measuring viscosity based on the Stokes-Einstein relationship:

$$D = 6\pi\eta a. \tag{18}$$

The τ_c obtained by measuring the rates of T_1 for each chemical group in the molecule should have the same value when the molecule is subjected to isotropic rotation. In fact, various correlation time values can be observed, and this proves the existence of internal motions in the molecule [4–6].

1.3.2. The Lipari-Szabo model-free approach

In liquids, molecules are subject to rotational motion around the symmetry axis, and individual groups of molecules demonstrate internal movement. A correlation function for this complex motion of the $\vec{R}_{IS}$ vector was derived in reference [9]. The model assumed that the total

rate of the rotational movements is equal to the sum of the rates of the entire molecule (overall rotation—isotropic rotation) and internal rotations:

$$\frac{1}{\tau_i} = \frac{1}{\tau_{i_{\text{all}}}} + \frac{1}{\tau_{i_{\text{inter}}}}, \tag{19}$$

where $\tau_{i_{\text{all}}}$ is the time of isotropic rotation of the entire molecule, and $\tau_{i_{\text{inter}}}$ is the time of the internal isotropic rotation.

According to this model, the rate of T_1 is dependent on the complex motion coefficient C_1[9]:

$$C_1 = \left[1 - \frac{3}{4}\left(\sin^4\beta + \sin^2 2\beta\right)\right], \tag{20}$$

where β is the angle between the axis of rotation and the vector $\vec{R_{IS}}$.

The coefficient C_1 can take any value between 0 and 1 (0> C_1> 1). When $C_1 = 1$, there is no internal movement, when C_1 <1, the vector $\vec{R_{IS}}$ is subject to the movement [9].

1.3.3. Spin-spin relaxation process

The spin-spin relaxation process is associated with losing the phase coherence via the nuclear spin system, which leads to the loss of the $\vec{M_{xy}}$ vector. The effectiveness of the process depends on the rate of the molecular reorientations. In viscous liquids and solids, molecular reorientation is slow, it either takes a few microseconds or it does not occur at all [2]. The strength of magnetic field comes from the $\vec{\mu}$ moments, decreases as the distance between the spins increases. Thus, only the nearest nuclei have a significant contribution to the B_{loc}field. Therefore, from the position of the individual spins, the strength of B_0 field in which they exist differs in the range of B_{loc}, and it may increase by several Gauss. The consequence of this phenomenon is that the resonance frequency of the spins will also be different [1]. Spins can transfer absorbed energy to other spins that are located at a lower state of energy. The rate of T_2 time determines a spin's lifetime at a given energy state. This phenomenon is associated with the broadening of quantum states, which is explained via the Heisenberg uncertainty principle [3]:

$$\Delta\varepsilon t_e \geq \frac{\hbar}{2}. \tag{21}$$

The shorter is the spin's lifetime, the greater the broadening of the quantum states. Therefore, the transverse relaxation time is related to the width of the resonance signal [1, 3]. The dependency of the half-width of the resonance signal $_{1/2}$ and the relaxation time T_2 is

$$\Delta\nu_{\frac{1}{2}} = \frac{1}{2\pi T_2}. \tag{22}$$

The values of the T_2 relaxation times in liquids are similar to the values of the T_1 times and they are relatively long; however, T_2 cannot be greater than T_1[1].

1.4. Spin-spin couplings

The interaction between $\vec{\mu}$ moments, located in the magnetic field B_0, is known as spin-spin coupling J (scalar coupling). Each nucleus interacts with every other nucleus through their valence electrons, and the value of the coupling J depends on the gyromagnetic ratio and the distance between the coupling nuclei (number of bonds). The consequence of the interaction (attraction or repulsion of the moments $\vec{\imath}$) is the splitting of the quantum states (discrete spectrum). Thus, a given multiplet is found on the spectrum and the distance between the split signals is equal to J. In general, if the proton n is coupled with the other protons, then $(n + 1)$ signals are obtained in the multiplet [1]. Thus, the methyl protons (CH_3) coupled with the two protons of the CH_2 group cause the splitting of the resonance signal on $(2 + 1)$ peaks. In multiplet, the intensity of the signals can differ, and this can be determined using Pascal's triangle. These rules go into effect only if the differences between the chemical shift ranges and the value of spin coupling J are sufficiently large [3].

The spin-spin coupling J of spin Y and spin X can provide a relaxation mechanism for spin Y if spin X undergoes relaxation with time T_1. Spin Y is subjected to a fluctuating field due to the rapid spin X reorientation [1].

1.4.1. Amplifying the signals via polarization transfer

In NMR, the polarization transfer method, or the spin population transfer, is used to amplify the weak resonance signals, for example, in the ^{13}C spectra. The intensity of the signal is directly proportional to the difference between the N_1 and N_2 spin populations at energy levels. The N_1/N_2 ratio fulfils the normal Boltzmann equilibrium between the spin states. The greater the B_0 field, the greater the difference between the spin populations, and this depends on the ratio of the γ of the spins [10]. The nuclei ^1H and ^{31}P have large values, hence, the resonance signals are easier to observe than a signal from ^{13}C nuclei. The use of selective pulses of B_1 field might increase signal intensity of the spins in coupled systems. In the case of a system in which a sensitive nuclei A (proton) is coupled with an insensitive nuclei X (^{13}C) in ^{13}C spectra, signals with a coupling value of J(C, H) = 209 Hz (e.g., for $^{13}CHCl_3$) are obtained [10].

Amplifying the parameter signal p may be represented as follows [10]:

$$p = 1 + \frac{\gamma_A}{\gamma_X} \vee p = 1 - \frac{\gamma_A}{\gamma_X}. \tag{23}$$

1.4.2. Nuclear Overhauser effect (NOE)

The nuclear Overhauser effect is a double-coupled nuclei resonance, which results in a change in the signal intensity (typically an increase). Intramolecular and intermolecular factors have an impact on the value of signal amplification [11]. The theoretical maximum value of the signal amplification, in the case of coupling of ^1H and ^{13}C nuclei and dipole-dipole relaxation, is 2.989. In fact, the value can change from 1 (which means no gain) to a maximum theoretical value [10]. Because dipole-dipole relaxation is the major relaxation

pathway for protons and the carbons that are directly bonded with protons, the intensity of resonance signals corresponding to them will be more than the intensity from other nuclei. Thus, the spectrum will show signals with various intensities [3]. Therefore, the proton-decoupled resonance technique is used for ^{13}C nuclei. The application of the proton-decoupling method and the NOE effect makes it possible to amplify the signal by up to 200% [10].

The NOE effect can also be observed in the ^{1}H NMR spectroscopy, when two protons, H^{α} and H^{β}, are not directly bonded, but they are sufficiently close to each other. If the signal from H^{α} is gained, then the intensity of the signal corresponding to H^{β} will also increase about 45% [10]. Two mechanisms are responsible for the amplification of the signal, which causes the transfer of polarization:

- dipole-dipole interaction through space and
- chemical exchange (in the two spins system *AX*, the nucleus *A* is polarized and then the polarization is transferred from *A* to *X* with the exchange constant *k*).

1.5. Detection of NMR spectra and NMR spectra parameters

After the discovery of the phenomenon of NMR in solids, it was found that this phenomenon can also be observed by treating the sample with a sequence of short pulses of B_1 field at resonance frequency [12]. After that, the sample can induce alternating voltage with frequency ω_0 in the coil. An increase in the coil-alternating current is observed as a signal of free induction decay (FID).

The pulse duration is given by the following formula [1]:

$$t_i = \frac{\theta}{\gamma B_1}. \tag{24}$$

The selected pulse rotates $\vec{M}$ vector by a given angle θ. The most commonly used pulses are the ones that rotate the $\vec{M}$ vector about 90° ($\pi/2$) or 180° (π) (**Figure 6**). The duration time of the pulses ranges from 1 to 100 μs [3].

The shape of the FID signal is a fading oscillation curve as a function of time. This function is archived in the acquisition time of approximately 1 s. Then, using Fourier transformation, the periodic changes in time are converted to the frequency spectrum. The advantage of using this method is that it enables the fast recording of the spectrum as well as accumulation and averaging, which increases the signal-to-noise ratio [1].

1.5.1. Chemical shift

The chemical shift is the most common parameter analyzed in the ^{1}H NMR spectra. This is due to the fact that the distribution of electrons in the molecule is varied, so the different chemical groups of the same molecule have a different screening constant [1, 3]. Consequently, the same nuclei require a different B_0 field to achieve a resonance condition at a

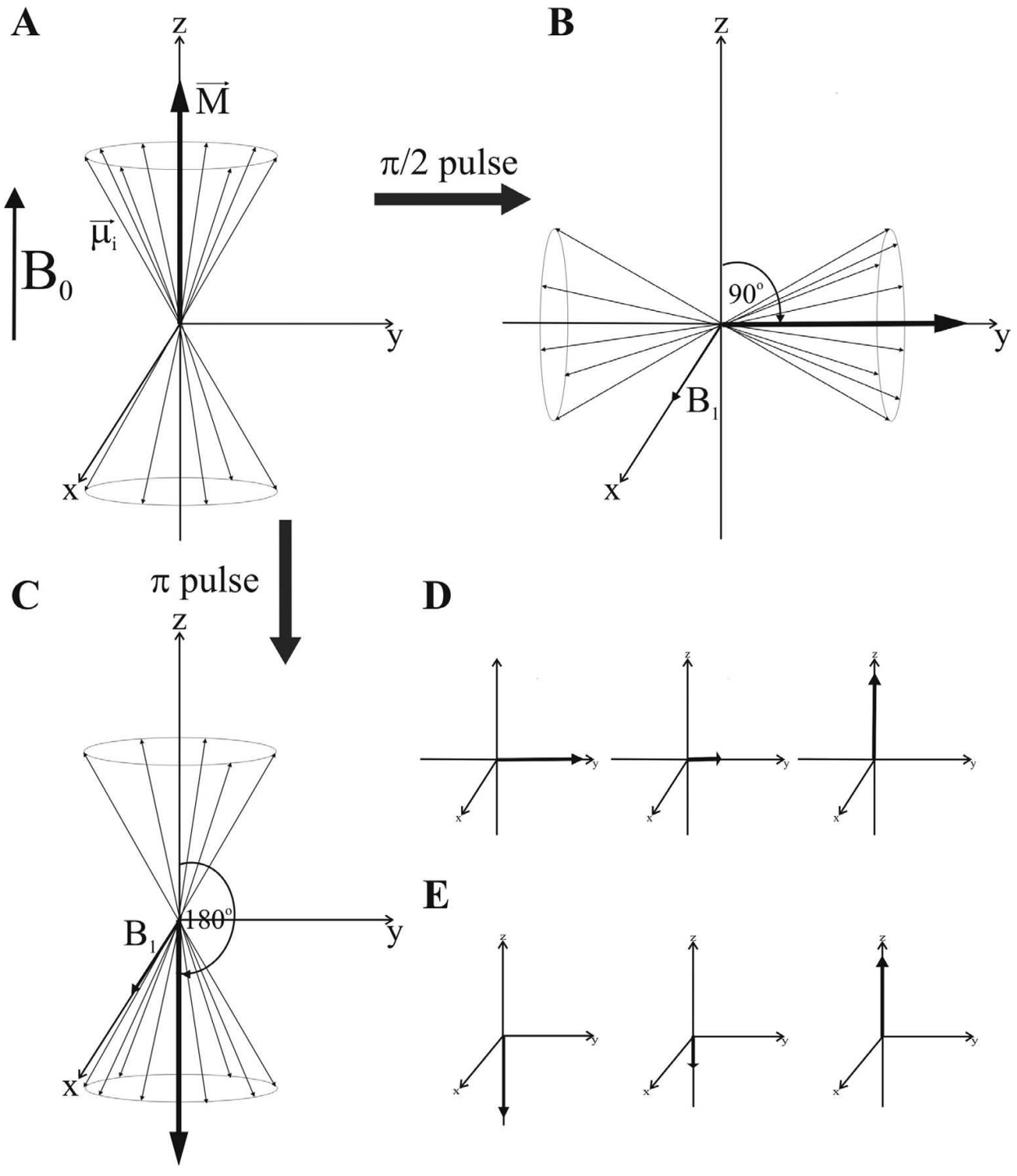

Figure 6. The B_1 field pulses rotate the $\vec{M}$ vector about (B) 90° ($\pi/2$) and (C) 180° (π); (A) the equilibrium state; the evaluation of the $\vec{M}$ vector and return to the equilibrium state in (D) the case (B) and (E) the case (C).

predetermined frequency ω_0.In this situation, the resonance condition must take the following form [1]:

$$B_{\text{ef}}(\text{ofsample}) = B_{\text{st}}(\text{ofstandard}) \tag{25}$$

Thus, the effective field acting on the nucleus must satisfy the following equation [1]:

$$B_{\text{ef}} = B_0(1-\kappa), \tag{26}$$

where κ is the screening constant that is a measure of the density of the electron cloud around the nucleus.

Substituting formula (26) to (25), we get

$$B_0(1-\kappa) = B_{\text{st}}(1-\kappa_{\text{st}}). \tag{27}$$

Assuming, that $(1-\kappa) \approx 0$, because κ is the order of 10^{-6}–10^{-2}, so $\kappa \ll 1$, we then get

$$\frac{B_{\text{st}} - B_0}{B_{\text{st}}} \approx \kappa_{\text{st}} - \kappa = \sigma, \tag{28}$$

where σ is the chemical shift.

However, in the given B_0 field the frequency changes ω_0, and then σ can be presented in the following form [3]:

$$\sigma = \frac{\nu - \nu_{\text{st}}}{\nu_{\text{st}}} \cdot 10^6 \left[\text{ppm}\right]. \tag{29}$$

As the physical parameter used to analyze ^{1}H NMR spectra, σ is defined as the difference between the positions of the sample and standard signals [1]:

$$\sigma = (\nu - \nu_{\text{st}}) \cdot 10^6 \left[\text{ppm}\right]. \tag{30}$$

The measurement range for hydrogen nuclei is about 15 ppm, which is about 3–10% of the spectroscopic range of other magnetic nuclei.

1.5.2. Presence of paramagnetic ions as a factor affecting a value of σ

During the interaction between metals, such as Eu^{3+} or Pr^{3+}, and molecules containing oxygen or nitrogen atoms, metal ions increase their coordination number and form unstable associations [1]. This changes the chemical environment of the protons as well as the dipolar interactions between the unpaired electrons of the metal ions and the protons. This causes a change in the chemical shifts of hydrogen. The value of σ depends on the distance between the proton and the paramagnetic ion, and the value decreases as the distance increases [1].

Paramagnetic ions are used to distinguish the signals assigned to the choline groups of phospholipids. The most frequently used ions are those from the lanthanide group [13]. The concentration of paramagnetic ions added to the external environment of liposomes varies and is unique to each ion. If the concentration is too great, it could broaden all NMR spectra due to the dominant paramagnetic interactions [14].

1.5.3. Intensity of the signal

The intensity of the signals in the ^{1}H NMR spectra is a measure of adsorption, and it is proportional to the number of protons that induced the signal [1]:

$$I = \left(1 + \gamma^2 B_1^2 T_1 T_2\right)^{\frac{1}{2}}. \tag{31}$$

The above formula takes into consideration the relaxation times of different protons in the molecule, and the strength of B_1 field. The physicochemical analysis of the NMR spectrum assumed that the area under the obtained signal is proportional to the number of protons inducing the signals [3]. Therefore, based on the measured area under the signal, the relative number of the protons in the molecule can be determined. Sometimes, the determined relative number of the protons in the molecule is not equal to the number of the protons resulting from the molecular formula. This usually occurs when oxygen, nitrogen, or sulfur are present in a molecular structure; in such a case, the proton may be exchanged for deuterium from the deuterated solvent [3].

1.5.4. Chemical shift anisotropy (CSA)

The ^{31}P lineshape is directly related to the CSA tensor and to the orientation of lipid molecule (relative to the B_0 field) [15]. The value of CSA depends on the phosphate group motion and the temperature. The ^{31}P spectra exhibit a characteristic narrow peak ($\sigma_\perp$—high-field maximum; isotropic part) and a low-field shoulder ($\sigma_\parallel$—anisotropic part). The CSA can be calculated using the fallowing formula [16]:

$$\Delta\sigma = 3\left(\sigma_\parallel + \sigma_\perp\right), \tag{32}$$

where $\sigma_\parallel$ and $\sigma_\perp$ are the values of ^{31}P shielding of the lipid molecules, oriented parallel or perpendicular relative to the magnetic field.

The value of CSA for multilamellar vesicles (MLVs) is about 40–50 ppm, and depends from the size of liposome. For small unilamellar vesicles (SUVs), the CSA value may decrease to 10 ppm [15].

1.6. Two-dimensional (2D) NMR spectra

The two-dimensional NMR experiments are most often used to determine the third and fourth structure of macromolecules.

1.6.1. Two-dimensional correlation spectroscopy (COSY) and total correlation spectroscopy (TOCSY)

The 2D homonuclear (H,H)-COSY experiment showed that the spectra with ^{1}H chemical shifts along the axes were correlated with each other [10, 17]. The pulse sequence of the COSY experiment is shown in **Figure 7A**. In the COSY spectra, the diagonal and cross peaks are visible and they always differ by 90^{o}.

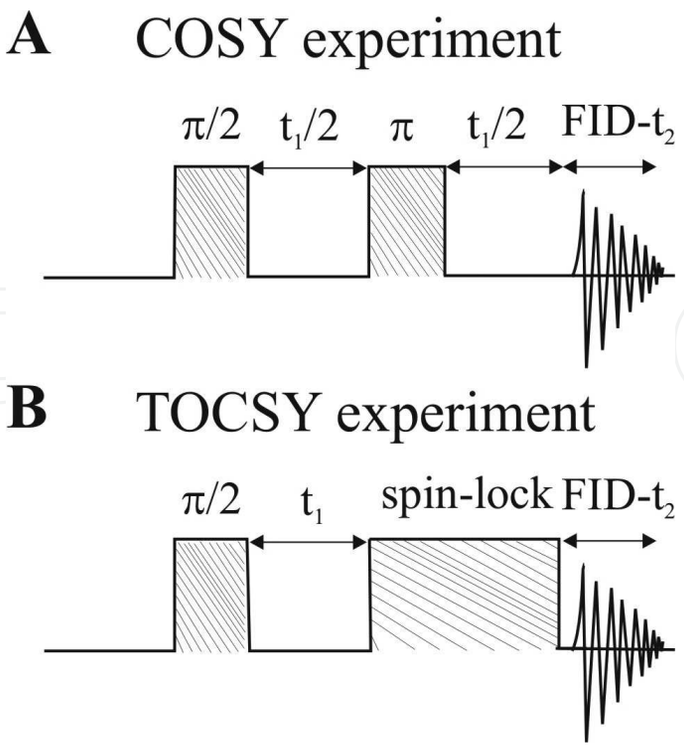

Figure 7. The pulse sequence of (A) the COSY experiment and (B) the TOCSY experiment; t_1 is a time between pulses; t_2 is an acquisition time; π and $\pi/2$ are pulses; spin-lock is a time of the spin states mixing.

When the system of two spins corrects the phase, the absorption signal appears as the cross peak, while the dispersion signal (incorrect phases) appears as the diagonal peak. The cross peaks in the horizontal and vertical directions are the absorption signals with positive and negative amplitudes [10]. When a proton is coupled with more than one proton, the diagonal peak is seen in the corner and it occupies more than one square. This simple rule of spectrum analysis makes the COSY technique an ideal tool for evaluating the ^{1}H spectra. The COSY spectra reveal information about the scalar coupling of protons within a few bonds [10, 17]. One disadvantage of the COSY method is that the cross peaks overlap with the diagonal signal when the chemical shift differences between the coupled nuclei are too small [10]. The 2D homonuclear (H,H)-TOCSY experiment is similar to the COSY experiment, but it exhibits the peaks from all scalar-coupled protons from the spin system [10, 17]. The pulse sequence of the TOCSY experiment is shown in **Figure 7B**. The method used to analyze the TOCSY spectra is similar to the method used to analyze the COSY spectra.

1.6.2. Rotating frame nuclear Overhauser enhancement spectroscopy (ROESY)

The nuclear Overhauser enhancement spectroscopy (NOESY) and ROESY techniques reveal information about the dipole-dipole-coupled protons and the transfer of polarization (the cross-polarization effect) [10, 17]. Usually, the ROESY experiment is used when the studied molecules are large. Then, the dipole-dipole relaxation is less effective because the rotation of the molecule is slow (long τ_c time), which extends the T_1 time [10]. Thus, the ROESY method is more convenient, because it ensures that the NOE effect will be positive [18, 19]. The pulse sequence of the ROESY experiment is shown in **Figure 8**.

Both processes, that is, dipole-dipole interaction through space and cross-polarization, influence the relaxation pathway. The mechanism of magnetization transfer is schematically shown in **Figure 9**.

Dipole-dipole interactions strongly depend on the distance between the coupled protons. Thus, the cross peaks differ in size. The ability to detect the interactions through space and to

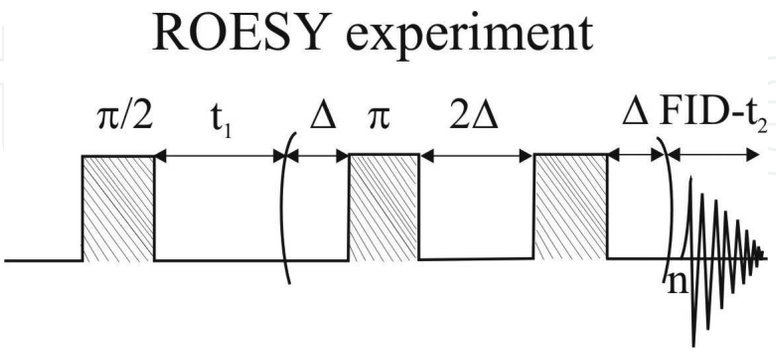

Figure 8. The pulse sequence of the ROESY experiment; t_1 is a time between pulses; t_2 is an acquisition time; π and $\pi/2$ are pulses; Δ is internal fixed time.

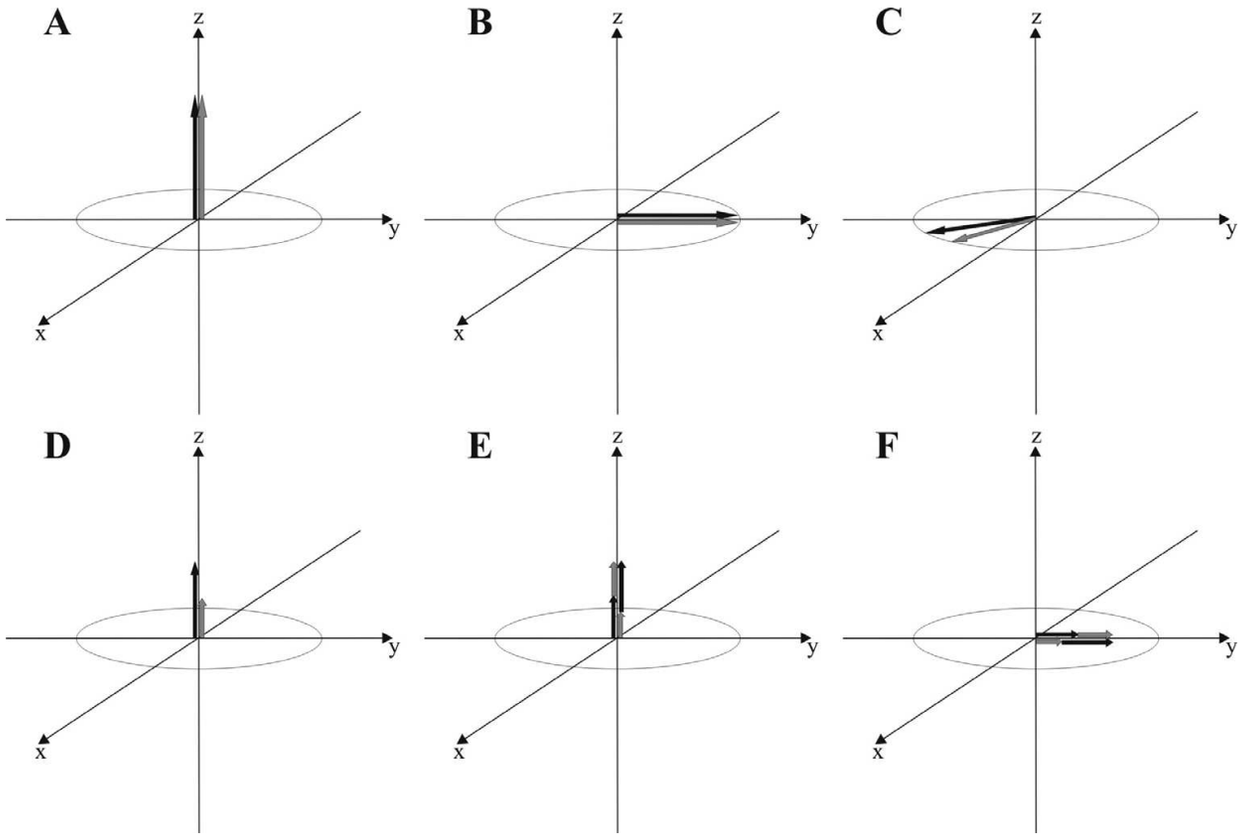

Figure 9. The evaluation of the magnetization vector M_A (black arrow) belonging to A protons and magnetization vector M_X (gray arrow) belonging to X protons. Spins A and X are close enough to interact through space. The diagrams from A to F show evaluation of the M_A and M_X vectors after two gradient pulses ($\pi/2$). The small contreating arrows superposed at the ends of the vectors represent the portion of the magnetization that is transferred from the nuclei of the other sort by cross-polarization during mixing time Δ.

http://dx.doi.org/10.5772/intechopen.68522

obtain general information about the distance between interacting protons provides valuable data about the stereochemistry of a molecule [10].

2. NMR studies of liposomes

The NMR spectra of liposomes differ from typical solution-NMR spectra. It is due to the specificity of lipid aggregates. The size of liposomes, hydration level, and the packing regime of lipid molecules in such structures have an influence on the NMR spectra.

2.1. Analysis of the ^{1}H NMR spectra

MLVs are not suitable for measurements using ^{1}H NMR method due to the large number of lipid bilayers and the large size of the liposomes. In this case, the signals in the ^{1}H NMR spectra are drastically broadened, and it is impossible to analyze any of the physical parameters of the spectrum. Even the signals on the spectrum of SUV/LUV are slightly broadened, and the broadening is not great enough to preclude spectrum analysis. This is due to the fact that liposomes are a kind of lipid aggregate, which distinguishes them from any substance which is soluble in water. From the physical point of view, this kind of sample is neither a homogeneous liquid nor a solid. The diffusion of water molecules and various ions through the lipid bilayer is the basic phenomenon that can be examined by the ^{1}H NMR spectra. The observation of this process is possible, thanks to the use of paramagnetic ions. It changes the chemical environment and the screening constant of each proton from the outer layer, which changes the σ values. Consequently, the choline group signal is split (δ) into two signals and it is assigned to the protons from the outer and inner layers of the liposome (**Figure 10**).

The type and concentration of used lanthanide ions is crucial, for example, if it is too great, the concentration of Eu^{3+} ions may exhibit as broadened ^{1}H spectra or they may even destroy the membrane structure. This effect is associated with the properties of the Eu^{3+} ions, which interact to the same extent with the hydrophilic and hydrophobic part of the liposome membrane. Moreover, the signal corresponded to water is broadened, which means that the Eu^{3+} ions also interact with the water molecules from the hydration shell of the liposome [14]. Thus, Pr^{3+} ions are most often used, which can split the choline signals within a few ppms without the effect of broadening the signals. The preferred concentration of Pr^{3+} ions ranges from 4 to 7 mM [20].

The split signals showed the different intensities. Since the area under a signal is directly proportional to the number of protons that induce the signal, a more intense signal is assigned to the protons from the outer layer and the lower intensity signal is assigned to the protons from the inner layer. This phenomenon is related to the asymmetric distribution of the lipid molecules in each layer. The splitting of the choline group signal creates new possibilities for research. The ratio of the area under the signal corresponds to the outer layer and the area under the signal corresponds to the inner layer (I_o/I_i); this provides information about the size of liposomes (**Figure 11**) [13, 20].

The splitting of the choline signal also offers the possibility to observe the ion transport through the membrane, since every change in the chemical environment of the protons from

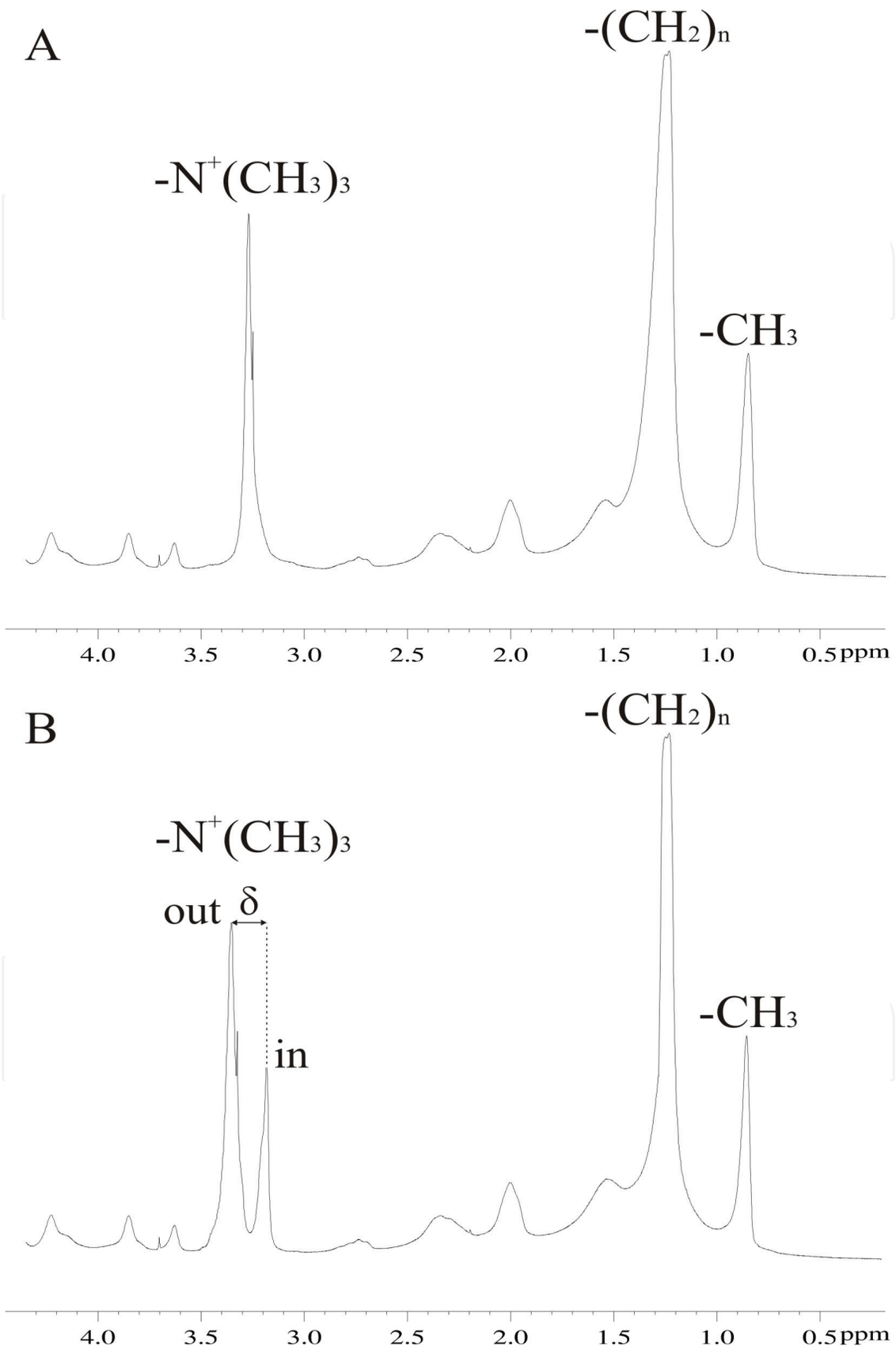

Figure 10. The characteristic ^{1}H spectra of egg-lecithin SUV (A) before and (B) after addition of 5 mM Pr^{3+}ions.

http://dx.doi.org/10.5772/intechopen.68522

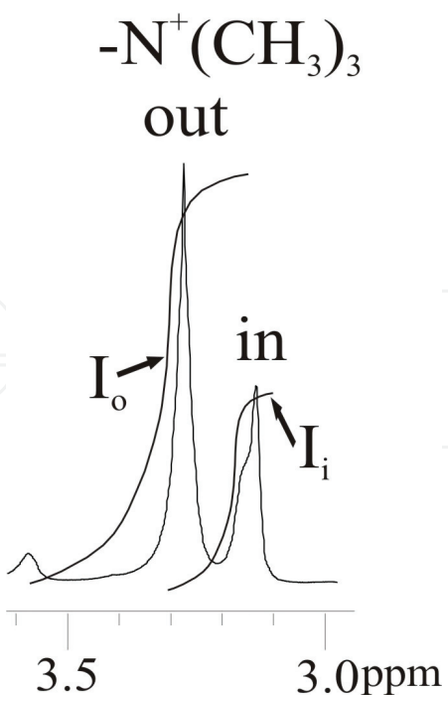

Figure 11. The measure of the area under the signals (integral of the signal) assigned to the protons from the choline groups.

the outer layer and the inner layer will be visible as a change in the σ of the signals. The value of the δ increases as the difference between the chemical environment of the protons from the inner and the outer layer increases [20, 21]. It is very important to maintain a constant temperature and pH for the sample during this kind of experiment because the binding of metal cations is dependent on both of these parameters [22]. The effect is clearly seen in the ^{1}H spectra of PE/PS/PC (phosphatidylethanolamine/phosphatidylserine/phosphatidylcholine) SUV (**Figure 12**).

The splitting of the choline groups is caused by 5 mM of the Pr^{3+} ions. Because the Pr^{3+} is associated only with the outer layer of a liposome, it is easy to observe the changes caused by the diffusion of Ca^{2+}ions in the distance between the splitting signals and the intensity. The value of δ decreased as the concentration of the Ca^{2+} ions increased inside the liposome [21]. The intensity of the signals assigned to the choline groups changed because the fusion process occurred in the SUVs. Ca^{2+} ions are a well-known fusogenic reagent. The fusion process of vesicles caused the increase in their size. Thus, the difference in the intensity of the signals assigned to the choline groups decreased. The fusion process also had an impact on the increase in the concentration of the Ca^{2+} ions in the liposome [21]. In a similar way, it is possible to conduct the experiment with compounds that are adsorbed on the surface of liposomes. Studying the area under each signal may also provide information about the processes that occur in the hydrophilic part of the lipid bilayer.

The half-width of the signal is another parameter that can be analyzed in the ^{1}H NMR spectra (**Figure 13**). The $\Delta\nu_{1/2}$ of the signal is closely related to the dynamics of the chemical groups. The slower the movement, the greater the $\Delta\nu_{1/2}$ of the signal.

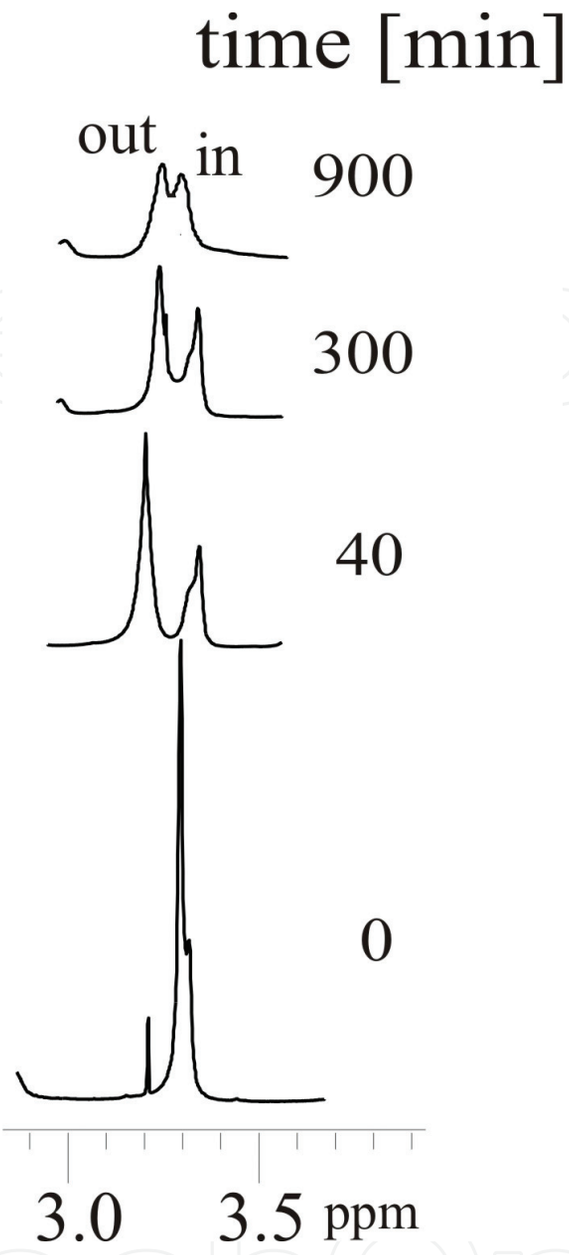

Figure 12. The time-dependent changes of ^{1}H resonance signals assigned to choline groups of PE/PS/PC SUVs after addition of 5.0 mM Pr^{3+} ions in the presence of Ca^{2+}/PS molar ratio of 2.0.

The processes that occur on the surface of the liposomes can cause the choline head to either become rigid or become more fluid, thereby slowing down/speeding up the rotational motion, which results in an increase/decrease in the $\Delta\nu_{1/2}$ of the signal. Additionally, cholesterol, antioxidants, and drugs contained in the liposomal membrane also may increase/decrease the fluidity of the membrane. For instance, the presence of azithromycin molecules increased the fluidity of 1,2-dipalmitoyl-*sn*-glycero-3-phosphocholine (DPPC) liposomes decrease of $\Delta\nu_{1/2}$ below the main phase transition temperature. However, amphotericin B rigidified the hydrophilic part (increase of $\Delta\nu_{1/2}$) of phospholipid bilayer, which increased the fluidity (decrease of $\Delta\nu_{1/2}$) of the hydrophobic core of PC membrane [16]. The opposite effect can be observed in the ^{1}H spectra of PC liposomes in the presence of polysialic acid

http://dx.doi.org/10.5772/intechopen.68522

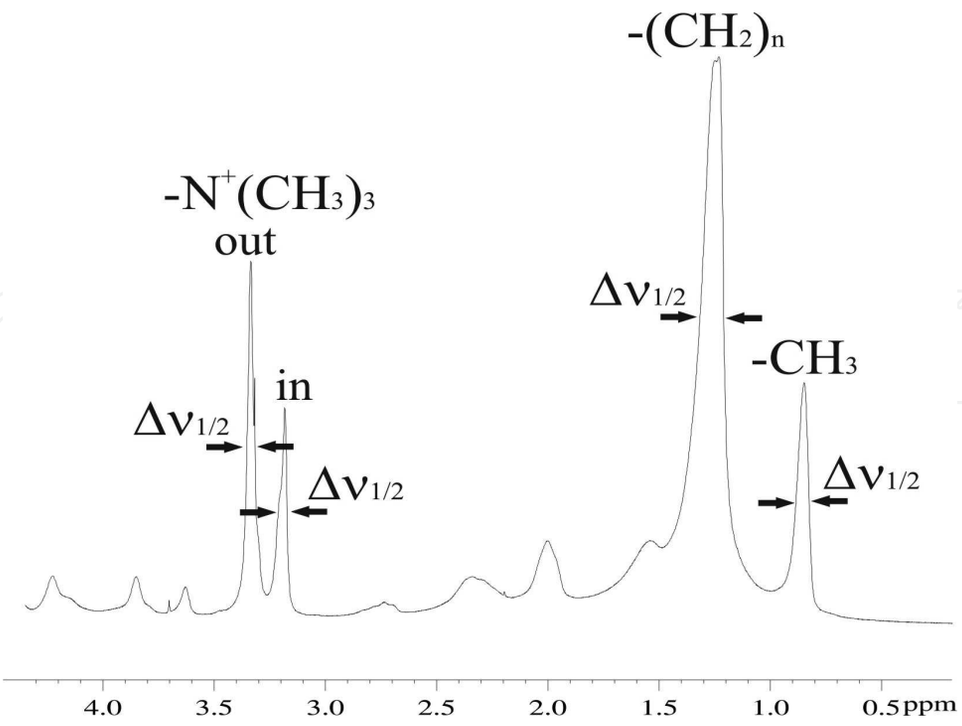

Figure 13. The $\Delta\nu_{1/2}$ of the signals from ^{1}H spectrum of egg-lecithin SUVs.

(**Figure 14**). The interaction of well-hydrated and anionic polysialic acid with the PC headgroups increased the fluidity of the hydrophilic part of the membrane and rigidified the hydrophobic core of the PC bilayer [23, 24].

The effect manifested as a decrease in the $\Delta\nu_{1/2}$ of the signal assigned to the choline groups from the outer layer of the liposome and as an increase in the $\Delta\nu_{1/2}$ of the signal assigned to the choline groups from the inner layer and to the $-(CH_2)_n$ and $-CH_3$ groups from the fatty acid chains. In fact, the observed effect is connected to the restricted motion of lipid molecules in the bilayer structure. The increase of the fluidity of the headgroups is connected to the increase of their rotational motion, their reorientation, and better hydration [17, 24]. The motion of the headgroups is restricted by the hydrophobic interactions, hydrogen bonding, and the intermolecular force between the lipid molecules. Thus, the presence of polysialic acid indicates that the strength of the PO_4^- and $N^+(CH_3)_3$ interactions is weakened. The increase of hydration (unrestricted motion) of headgroups and their reorientation causes the hydrocarbon chains to be more exposed to water molecules. Thus, the membrane polar-apolar interface is more hydrophobic [25].

Studies of liposomes using ^{1}H-NMR can also be conducted with various physical parameters, including temperature. The influence of temperature on the ^{1}H spectra manifests as an increase in the σ values of all the signals (**Figure 15**).

The resonance signals shift toward the direction of the lower magnetic field. This effect is typical for lipid bilayers [26]. The increase in temperature has an impact on the increase in the fluidity of the membrane. It manifests as a decrease of the $\Delta\nu_{1/2}$ of the signals. The ^{1}H NMR temperature-dependent studies may be used to analyze the properties of temperature-sensitive liposomes.

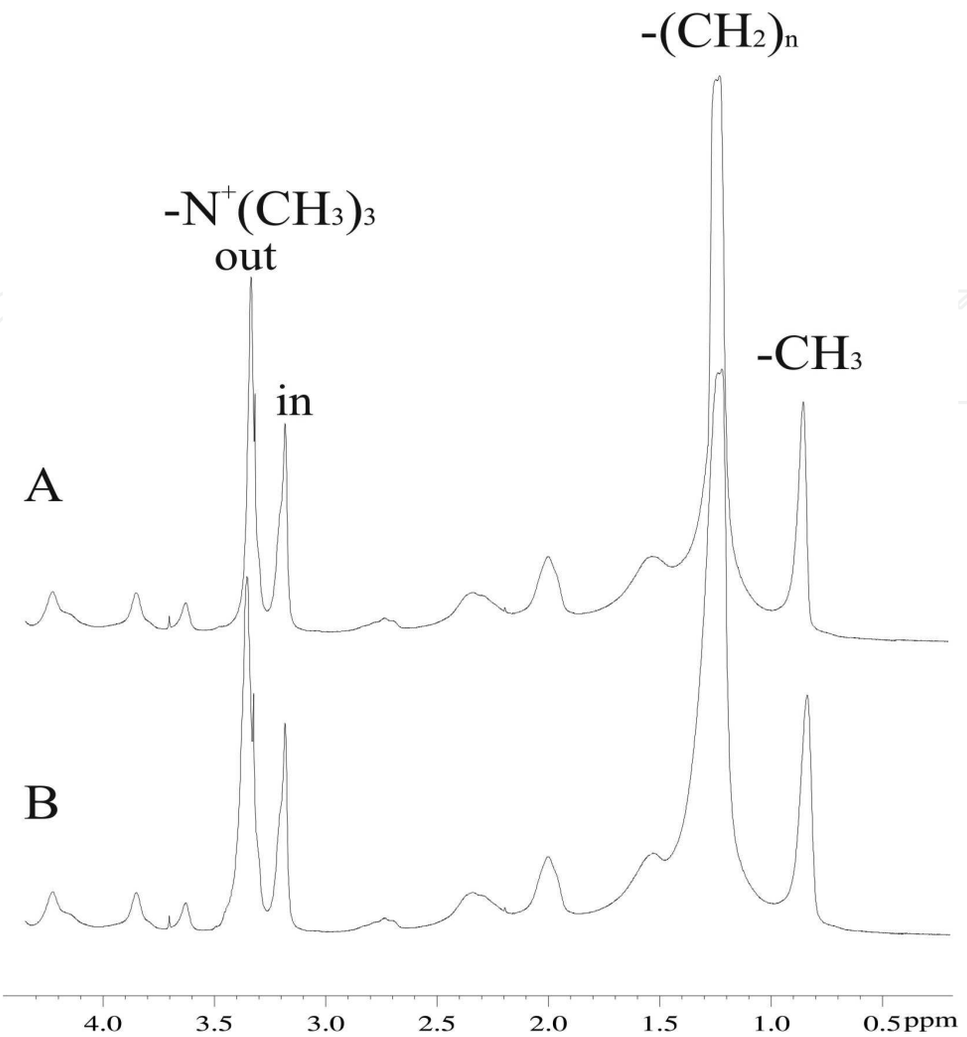

Figure 14. The effect of polysialic acid on changes of the PC SUVs membrane fluidity (the $\Delta\nu_{1/2}$ changes). (A) The ^{1}H NMR spectra of PC SUVs and (B) in the presence of polysialic acid.

The concept of using temperature-sensitive liposomes as drug carriers in local hyperthermia is based on the increase in their therapeutic effect, the ability to reduce drug toxicity for normal cells, and the increase in the permeability of the lipid bilayer at the proper temperature [26, 27]. The release rate of a drug depends on the temperature changes and the serum compounds (lipoproteins); thus, liposomes should be stable in serum and they should release drugs slowly under a proper temperature [28]. The ^{1}H spectra of PC and PC/octadecylamine liposomes (positively charged LUV) showed a narrowing of the resonance signals (decrease in the $\Delta\nu_{1/2}$) assigned to –N+$(CH_3)_3$, -$(CH_2)_n$, and –CH_3(**Figure 16**). The largest changes in the $\Delta\nu_{1/2}$ were observed for the signal corresponding to the fatty acid chains, –$(CH_2)_n$groups [26]. The effect was observed in temperatures ranging from 5 to 50°C.

Studies on changes of the splitting and intensity of signals assigned to choline groups revealed that the size of the liposomes increases [26]. In fact, the size of PC liposomes changed from 20–30 nm to 1 μm. Thus, as the temperature increases, the size of the PC liposome also increases. Additionally, when the temperature ranges from 30 to 40°C, the structure of the liposome

http://dx.doi.org/10.5772/intechopen.68522

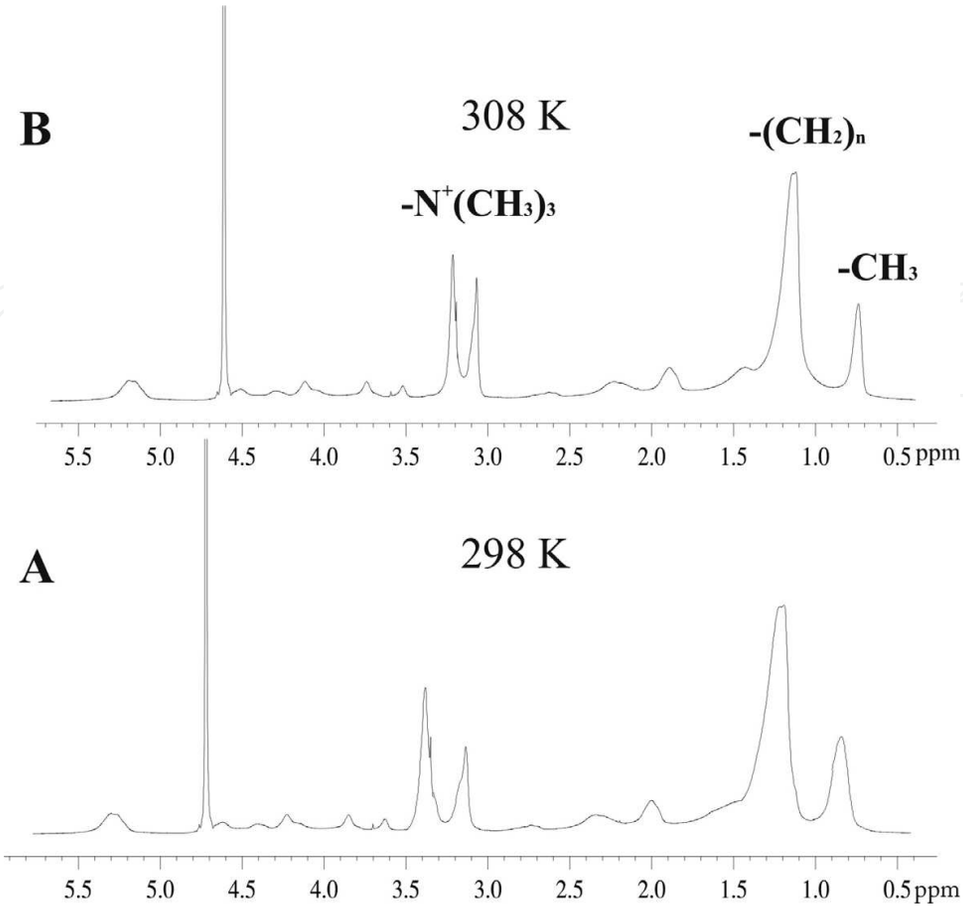

Figure 15. The influence of temperature on the ^{1}H resonance signals shifting. The ^{1}H NMR spectra of PC SUVs at (A) room temperature and (B) 308 K.

membrane is damaged; this makes the PC liposomes completely unstable and useless as thermosensitive drug carriers [26]. Quite the opposite effect was observed in the case of the PC/octadecylamine liposomes. The temperature had a smaller influence on the liposome size changes (from 20 to 60 nm), and the size was changed slowly. The PC/octadecylamine liposomes also seemed to be stable at temperatures ranging from 40 to 50°C [26]. At higher temperatures, the temperature-sensitive liposomes may aggregate or fuse, which makes it possible to transfer the drug to cells by fusion or via an endocytosis process in hyperthermia [26, 29].

2.2. Analysis of the ^{31}P NMR spectra

Liposomes can be composed of one or more kinds of phospholipids. Their molecular structure contains phosphorus atoms, which makes the ^{31}P NMR method extremely useful for studying them. Both MLVs and LUVs/SUVs can be studied using that method. In MLVs, the signal assigned to the phosphate groups is drastically broadened, and its shape is not like the Lorentzian function, unlike the SUVs/LUVs. The ^{31}P NMR spectra are mainly used to study the thermotropic properties of liposomes. The various phases change the structure of membrane, and there are specific transition temperatures for each lipid.

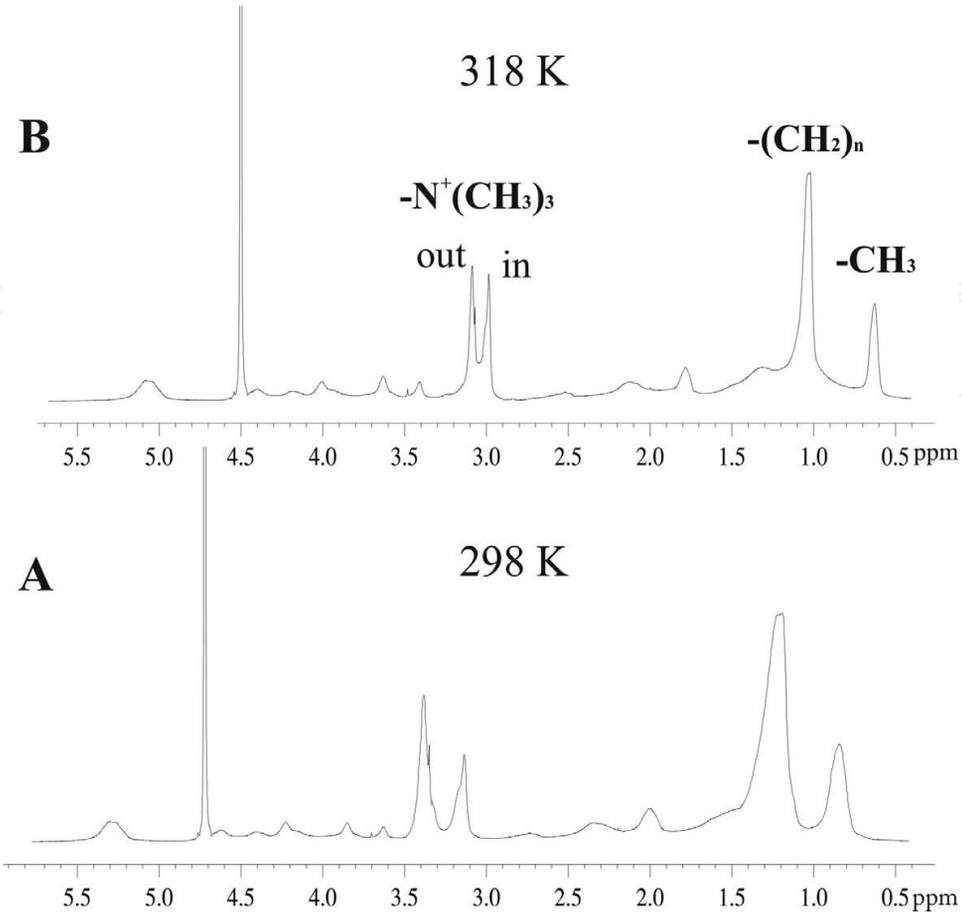

Figure 16. The ^{1}H NMR spectra of PC/octadecylamine liposomes at (A) room temperature and (B) 318 K.

The ^{31}P spectra of PC/Ch MLVs exhibited changes in the lineshape in the temperature range of 10–40°C. The characteristic ^{31}P lineshape of the L_α phase was observed before the phase transition. The monitoring of ^{31}P spectra at short temperature intervals led to observing the intermediate lineshapes between those characteristics for the L_α and H_{II} phases [21]. Substances that are either added to liposome membrane or are found in the liposomal environment can increase/decrease the phase transition temperature. For instance, this can be seen in the effect of the change of phase transition temperature caused by various drugs. The ^{31}P spectra of DPPC MLVs used in various concentrations of Piracetam showed that an additional narrow signal was assigned to the drug [30]. As the concentration of Piracetam increases, the intensity of the signal assigned to that drug also increases. The temperature studies showed that the main phase transition temperature of DPPC MLVs decreased in the presence of Piracetam. The results suggest that hydrophilic Piracetam molecules are associated with the hydrophilic part of the liposome membrane, which increases the fluidity of the membrane. Thus, the temperature of the main phase transition decreases [30].

The ^{31}P NMR method reveals information about the mobility of phosphate groups and about local order. Various substances impact the dynamics of the hydrophilic and hydrophobic part of the lipid bilayer. The number of narrow peaks in the ^{31}P spectra depends on the number of phospholipid types used to form the liposomes [31]. The effect is due to differences in the chemical surroundings of the phosphate groups in each type of phospholipid molecule. In the

^{31}P spectra, the splitting between the signals depends more on the averaged CSA motions than on an isotropic chemical shift [31]. It influences the value of chemical shift, and it may be difficult to assign the signals.

As previously mentioned, the effect of azithromycin on DPPC MLVs [16] was studied. Temperatures ranging between 35 and 45°C did not change the position of the narrow peak and CSA value, but the ^{31}P lineshape in the low-field shoulder was changed, and the presence of azithromycin in the external environment of the liposome decreased the CSA value. In fact, above 40°C, only a narrow peak stays in the spectrum because the CSA value is averaged to zero. The azithromycin caused an increase in the fluidity of the DPPC membrane below the temperature of the main phase transition [16].

When hydrophobic β-carotene is added to a lipid membrane, changes in DPPC membrane fluidity can also be observed. In temperatures above the main phase transition, β-carotene increases the fluidity of the DPPC MLV membrane, and in temperatures below the main phase transition, it decreases the fluidity of that membrane [32].

The opposite effect may be observed for PC MLVs in the presence of polysialic acid (**Figure 17**). In the temperature range of 10–30°C, the ^{31}P spectra show a narrowing of the isotropic part and broadening of the anisotropic part (increase in the CSA value) [23]. The increase of well-hydrated polysialic acid in the membrane increased the fluidity of the headgroups; this resulted in a decrease in the hydrophobic core fluidity.

The ^{31}P NMR spectra also are used to study the fusion process that occurs between liposomes. These types of experiments use fusogenic factors. The ^{31}P NMR is the best method for

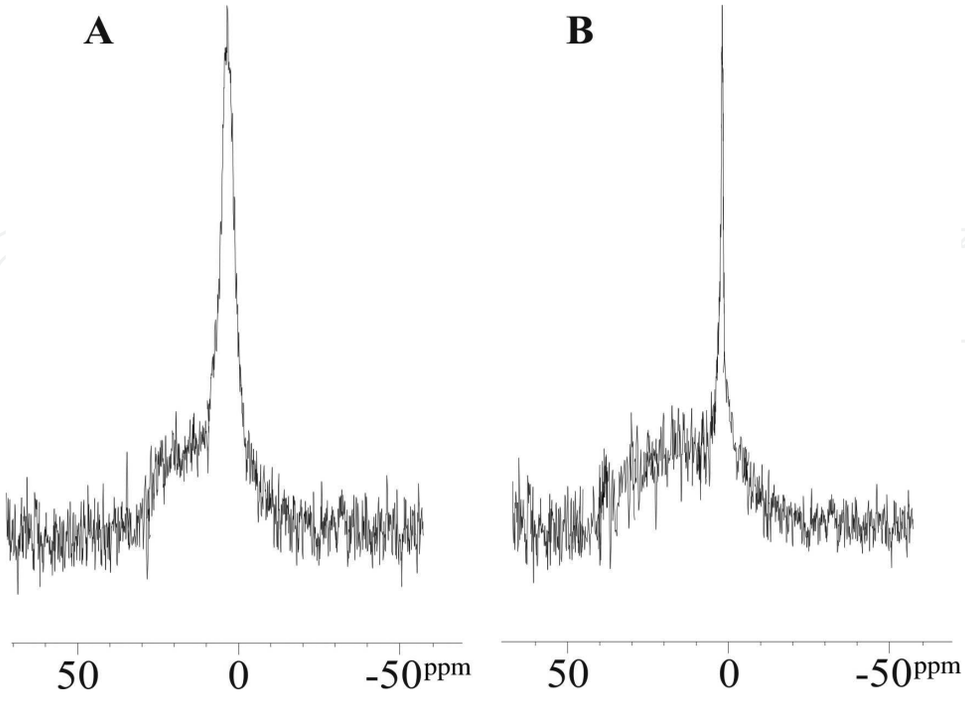

Figure 17. The effect of polysialic acid on ^{31}P NMR spectra of PC MLVs at room temperature. The ^{31}P spectra (A) before and (B) after addition of polysialic acid.

examining the fusion process because it has been proven that the fusion of two vesicles is accompanied by a transient structure, that is, the inverse hexagonal phase [29, 33].

The ^{31}P lineshape of PE/PS/PC MLVs showed changes with an increased molar ratio of Ca^{2+} ions (**Figure 18**). In fact, the Ca^{2+} ions are a well-known fusogenic factor. The characteristic lineshape for the H_{II} phase was obtained when the molar ratio of Ca^{2+}/PS was 2.0 [21]. It means that when the molar ratio of Ca^{2+}/PS is 2.0, the fusion process occurs.

The monitoring of changes in the ^{31}P spectra of PE/PS/PC SUVs after the addition of Ca^{2+} and Pr^{3+} ions showed that the signals were assigned to the choline groups from the inner and outer layers of the membrane. The obtained results revealed the decrease of δ-value and the intensity equalization of the signals corresponded to the choline groups [21]. The Pr^{3+} ions are only associated with the

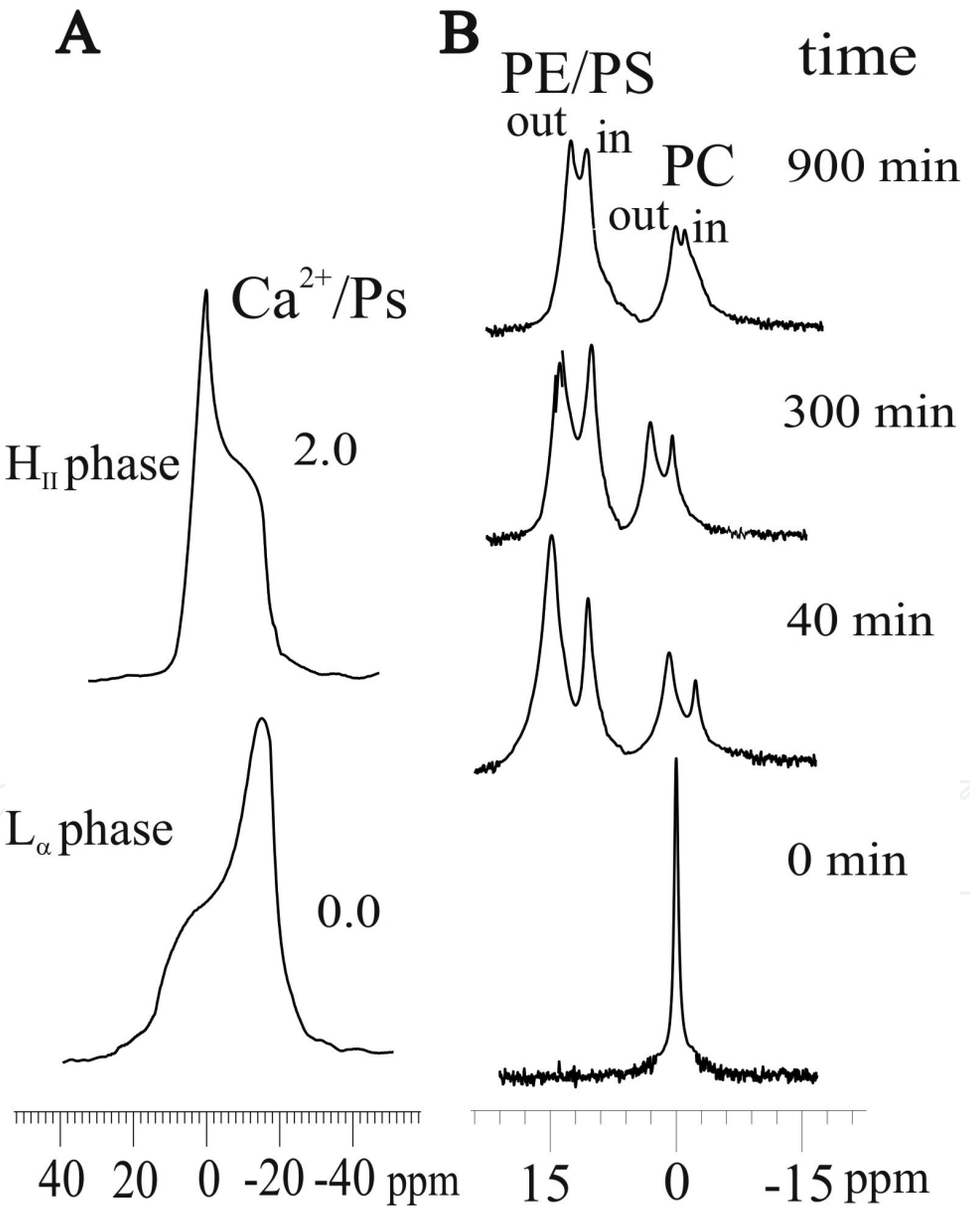

Figure 18. The 31P NMR spectra of PE/PS/PC liposomes; (A) the characteristic ^{31}P lineshape of MLVs in the L_α and H_{II} phase, (B) the time-dependent changes of LUVs after addition of 5.0 mM Pr^{3+} ions in the presence of Ca^{2+}/PS molar ratio of 2.0.

http://dx.doi.org/10.5772/intechopen.68522

outer layer of a liposome, while the Ca^{2+} ions are not (they can diffuse through the membrane). Thus, the obtained results suggest that during the transient phase (inversed micelle) the fusion process, the lipid molecule transition from the outer to the inner layer and the size of the liposome, increases [21]. These results also confirmed the topological model of the fusion.

2.3. Two-dimensional NMR spectroscopy

2D NMR spectroscopy is the most convenient technique for studying scalar and dipole-dipole couplings. The results obtained using the method are used to study the structure and stereochemistry of molecules [10].

2.3.1. COSY and TOCSY spectra

In the COSY spectra of the PC/octadecylamine SUVs, the signals from the protons coupled within a few of the chemical bonds are visible. The diagonal peaks corresponded to each proton cross-correlated with every other proton from spin system [17, 26]. **Figure 19** depicts the method used to analyze the COSY spectra.

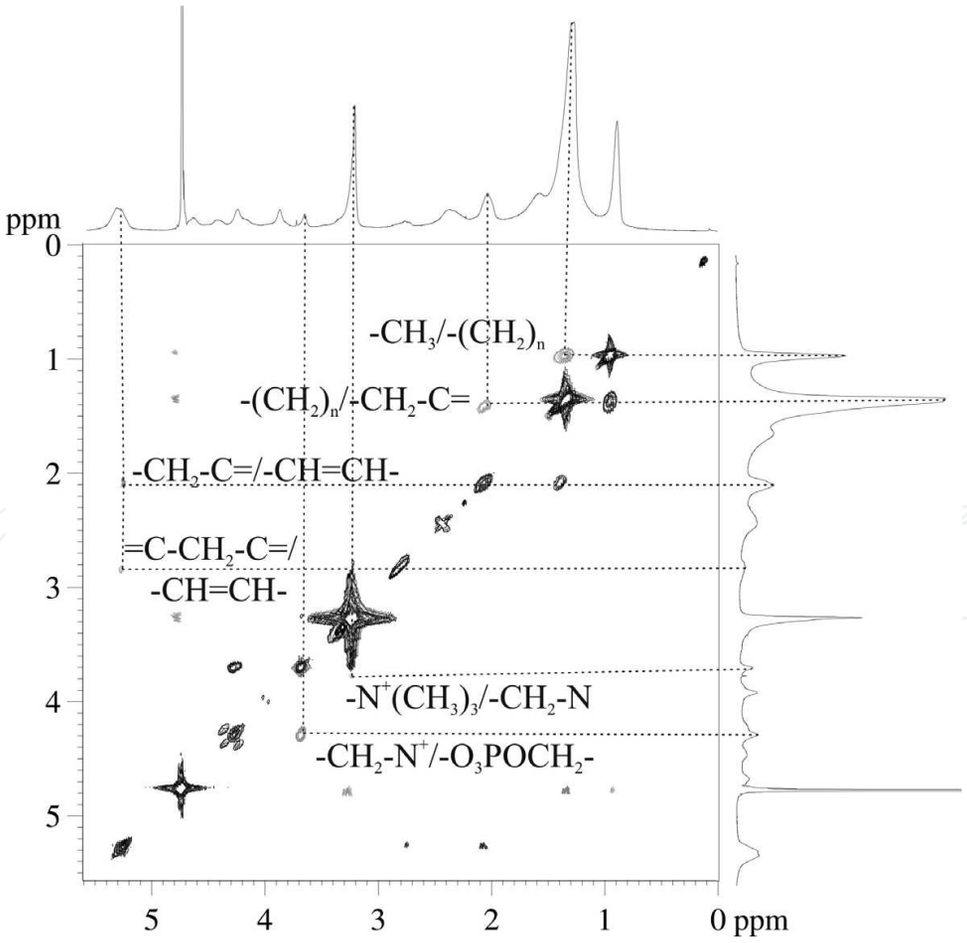

Figure 19. The COSY spectra of PC/octadecylamine SUVs. The cross peaks of scalar-coupled protons from the PC and octadecylamine molecules, and between protons from the PC/octadecylamine and water molecules (unsigned) are depicted in gray.

On comparing the TOCSY and COSY spectra of PC/octadecylamine SUVs, it is possible to determine the differences between them (**Figure 20**). In the TOCSY spectra, all the scalar-coupled protons in the PC molecule can be seen [17]. Both spectra also exhibit the cross peaks between the fatty acid chain groups from the hydrophobic core of the membrane and the water molecules. This is characteristic of well-hydrated membranes in the liquid crystalline phases [17, 26].

2.3.2. ROESY spectra

The ROESY spectra of the PC/octadecylamine SUVs reveal information about the protons coupled through space. Now, the diagonal peaks exhibit dipole-dipole interactions. The observed interactions may occur within one molecule or between neighboring PC molecules. The results also show the interactions between the hydrophilic part (headgroups) and the hydrophobic part (fatty acid chains) of the membrane (**Figure 21**) [17, 26]. The size of the cross-peak is directly proportional to the distance between the coupled protons. This dependency is clearly visible on the ROESY spectra of the PC/octadecylamine liposomes.

The 2D NMR technique is most often used to study the interactions between lipid molecules and substances added to the liposome membrane or to the external environment of liposome. To examine the nature of the interaction (either scalar coupling or through space), COSY/

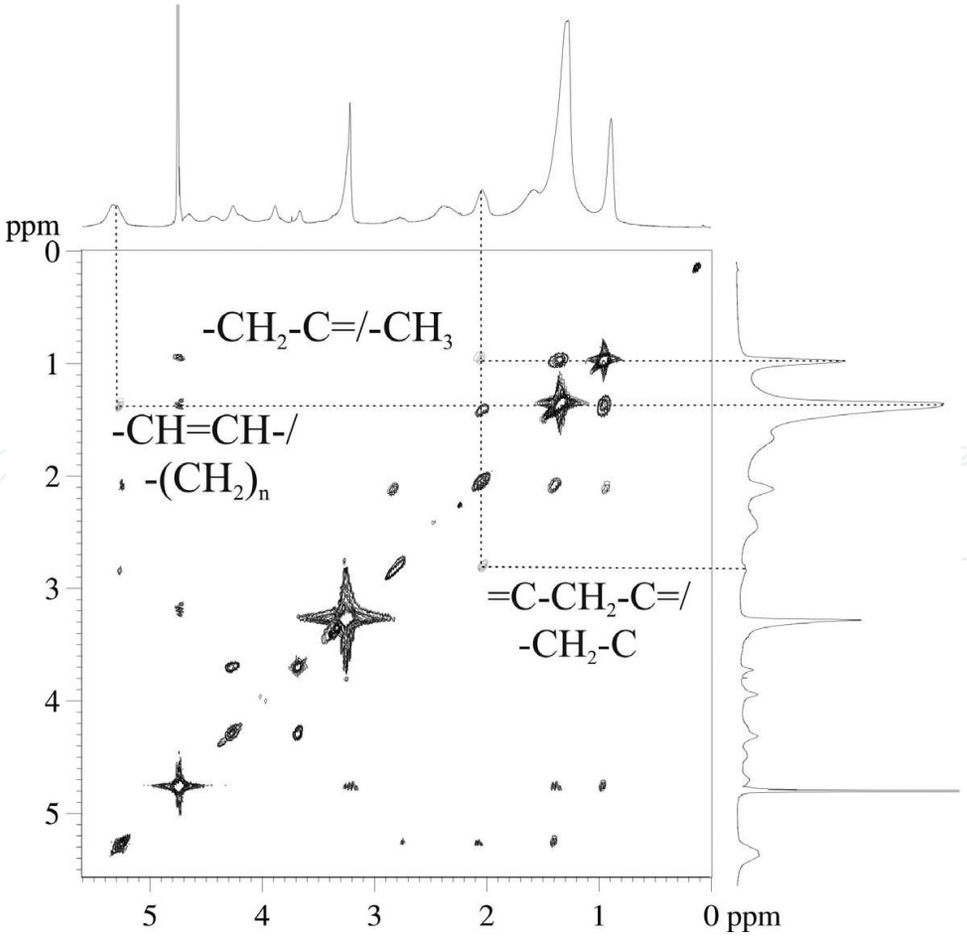

Figure 20. The TOCSY spectra of PC/octadecylamine SUVs. Only new cross peaks are depicted in gray.

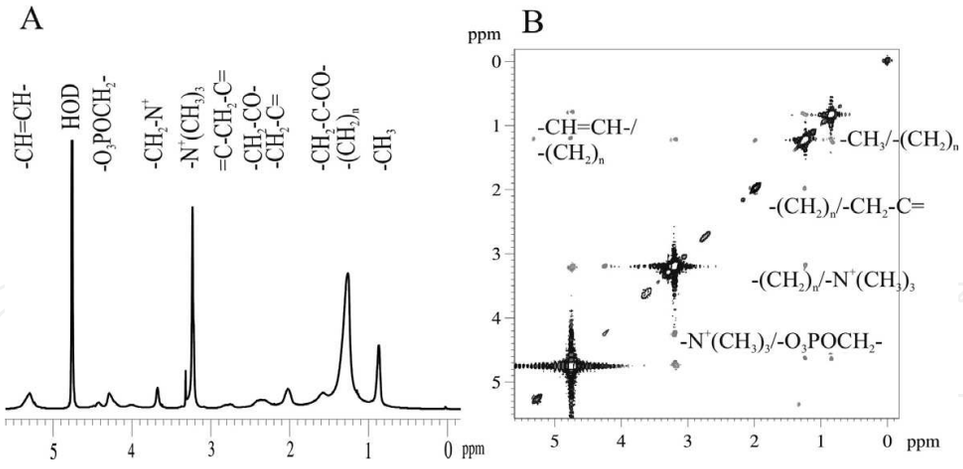

Figure 21. The ROESY spectra of PC/octadecylamine SUVs. (A) The full assigned ^{1}H spectra of the PC/octadecylamine liposomes; (B) The ROESY spectra of the PC/octadecylamine SUVs with assigned dipole-dipole interactions (in gray).

TOCSY or NOESY/ROESY experiments should be used, respectively. An example of this could be the ROESY spectra of PC/octadecylamine SUVs in the presence of sialic acid [17]. When comparing the ROESY spectra of sialic acid and PC/octadecylamine liposomes with PC/octadecylamine SUVs in the presence of sialic acid, it is easy to identify the new cross peaks due to interactions of the protons from the PC/octadecylamine and sialic acid molecules. While the interaction of sialic acid with the PC membrane has a considerable impact on membrane fluidity, the ROESY results only showed one cross peak between sialic acid and the PC molecules [17]. It is interesting to note that the dipole-dipole interaction occurs between the protons from the acyl group of sialic acid and the $(-CH_2)_n$ groups of the PC fatty chains. This result suggests that the other functional groups of sialic acid are well hydrated and, perhaps, the hydrophilic part of the membrane and sialic acid molecule interacts between their hydration shells. The obtained result also explains the strong influence that sialic acid has on decreasing the fluidity of the hydrophobic core of the membrane [17, 26].

Author details

Anna Timoszyk

Address all correspondence to: a.timoszyk@wnb.uz.zgora.pl

Department of Biotechnology, Faculty of Biological Sciences, University of Zielona Góra, Zielona Góra, Poland

References

[1] Hausser KH, Kalbitzer HR. NMR für Mediziner und Biologen. 1st ed. Heidelberg, Germany: Springer-Verlag Berlin Heidelberg; 1989. p. 246

[2] Latanowicz L. Dynamics of proton transfer in solution by NMR relaxation. Berichte der Bunsengeselleschaft für physikalische Chemie. 1987;**91**(3):237-242. DOI: 10.1002/bbpc.19870910314

[3] Lewitt MH. Spin Dynamics: Basics of Nuclear Magnetic Resonance. 2nd ed. New York, NY: Wiley; 2008. p. 740. ISBN 978-0-470-51117-6

[4] Abragam A. The Principles of Nuclear Magnetism. 5th ed. Oxford: Clarendon Press; 1983. p. 618. ISBN 9780198520146

[5] Bloembergen N, Purcell EM, Pound RV. Relaxation effect in molecular magnetic resonance absorption. Physical Review. 1948;**73**(7):679-692. DOI: 10.1103/PhysRev.73.679

[6] Kubo R. Note on stochastic theory of resonance absorption. Journal of Physical Society of Japan. 1954;**9**:935-944. DOI: 10.1143/JPSJ.9.935

[7] Gutowsky HS, Woessner DE. Nuclear magnetic spin-lattice relaxation in liquids. Physical Review. 1956;**104**:843-852. DOI: 10.1103/PhysRev.104.843

[8] Torrey NC. Nuclear spin relaxation by translational diffusion. Physical Review. 1953; **92**(4):962-973. DOI: 10.1103/PhysRev.92.962

[9] Lipari G, Szabo A. Model-free approach to the interpretation of molecular magnetic resonance relaxation in macromolecules.1. Theory and range of validity. Journal of American Chemical Society. 1982;**104**(17):4546-4559. DOI: 10.1021/ja00381a009

[10] Friebolin H. Basic One- and Two-Dimensional NMR Spectroscopy. 5th ed. New York, NY: Wiley; 2010. p. 442. ISBN 978-3-527-32782-9

[11] Overhauser AW. Polarization of nuclei metals. Physical Review. 1953;**92**(2):411-415. DOI: 10.1103/PhysRev.92.411

[12] Hahn EL. Spin echoes. Physical Review. 1950;**80**:580-594. DOI: 10.1103/PhysRev.80.580

[13] Gabrielska J, Gagoś M, Gubernator J, Gruszecki WI. Binding of antibiotic amphotericin B to lipid membranes: A ^{1}H NMR study. FEBS Letters. 2006;**580**:2677-2685. DOI: 10.1016/j.febslet.2006.04.021

[14] Schultze KD, Sprinz H. Electrochemical and NMR spectroscopic investigations of the influence of the probe molecule Eu(fod)$_3$ on permeability of lipid membranes to ions. Biochimica et Biophysica Acta. 2000;**1467**(1):27-38. DOI: 10.1016/S0005-2736(00)00193-0

[15] Leal C, Rögnvaldsson S, Fossheim S, Nilssen EA, Topgaard D. Dynamic and structural aspects of PEGylated liposomes monitored by NMR. Journal of Colloid and Interface Science. 2008;**325**:485-493. DOI: 10.1016/j.jcis.2008.05.051

[16] Fa N, Ronkart S, Schanck A, Deleu M, Gaigneaux A, Goormaghtigh E, Mingeot-Leclercq M-P. Effect of the antibiotic azithromycin on thermotropic behavior of DOPC or DPPC bilayers. Chemistry and Physics of Lipids. 2006;**144**:108-116. DOI:10.1016/j.chemphyslip.2006.08.002

[17] Timoszyk A, Latanowicz L. Interactions of sialic acid with phosphatidylcholine liposomes studied by 2D NMR spectroscopy. Acta Biochimica Polonica. 2013;**60**(4):539-546

[18] Sanders JKM, Hunter BK. Modern NMR Spectroscopy: A Guide for Chemists. 2nd ed. London: Oxford University Press; 1993. p. 328. ISBN 9780198555674

[19] Bax A, Grzesiek S. ROESY. In: Grant DM, Harris RK, editors. Encyclopedia of Nuclear Magnetic Resonance. 1st ed. West Sussex: Wiley; 1996. pp. 4157-4166

[20] Hunt GRA, Tipping LRH. A ^{1}H NMR study of the effects of metal ions, cholesterol and *n*-alkanes on phase transitions in the inner and outer monolayers of phospholipid vesicular membranes. Biochimica et Biophysica Acta. 1978;**507**(2):242-261. DOI: 10.1016/0005-2736(78)90420-0

[21] Osajca A, Timoszyk A. Application of ^{1}H and ^{31}P NMR of topological description of a model of biological membrane fusion. Acta Biochimica Polonica. 2012;**59**(2):219-224

[22] Amari L, Layden B, Rong Q, Geraldes FGC, de Freitas DM. Comparison of fluorescence, ^{31}P and ^{7}Li NMR spectroscopic methods for investigating Li^{+}/Mg^{2+} competition for molecules. Analytical Biochemistry. 1999;**272**:1-7

[23] Timoszyk A, Gdaniec Z, Latanowicz L. The effect of polysialic acid on molecular dynamics of model membranes studied by ^{31}P NMR spectroscopy. Solid State Nuclear Magnetic Resonance. 2004;**25**:142-145. DOI: 10.1016/j.ssnmr.2003.03.023

[24] Timoszyk A, Janas T. Effect of sialic acid polymers on dynamic properties of lecithin liposomes modified with the cationic octadecylamine. Molecular Physics Reports. 2003;**37**:67-70

[25] Walde P, Blöchliger E. Circular dichroic properties of phosphatidylcholine liposomes. Langmuir. 1997;**13**(6):1668-1671. DOI: 10.1021/la9610157

[26] Timoszyk A, Latanowicz L. Physical stability of temperature-sensitive liposomes. In: Bryjak M, Majewska-Nowak K, Kobsch-Korbutowicz M, editors. The impact of membrane technology to human life. 1st ed. Wrocław: Technical University of Wrocław Publishing; 2006. pp. 27-34. ISBN 83-7085-922-4

[27] Gaber MH, Hong K, Huang SK, Papahadjopoulos D. Thermosensitive sterically stabilized liposomes: Formulation and *in vitro* studies on mechanism of doxorubicin release by bovine serum and human plasma. Pharmaceutical Research. 1995;**12**(10):1407-1416. DOI: 10.1023/A:1016206631006

[28] Landon ChD, Park J-Y, Needham D, Dewhirst MW. Nanoscale drug delivery and hyperthermia: The material design and preclinical and clinical testing of low temperature-sensitive liposomes used in combination with mild hyperthermia in treatment of local cancer. Open Nanomedicine Journal. 2013;**3**:38-64. DOI: 10.2174/1875933501103010038

[29] Verkleij AJ, Bombers C, Gerritsen WJ, Leunissen-Bijvelt L, Cullis PR. Fusion of phospholipids vesicles in association with the appearance of lipidic particles as visualized by

freeze fracturing. Biochimica et Biophysica Acta. 1979;**555**:358–361. DOI: 10.1016/0005-2736(79)90175-5

[30] Lindberg G. Resialylation of sialic acid deficit vascular endothelium circulating cells and macromolecules may counteract the development of atherosclerosis: A hypothesis. Atherosclerosis. 2007;**192**(2):243-245. DOI:10.1016/j.atherosclerosis.2007.03.011

[31] Torchilin VP. Recent advances with liposomes as pharmaceutical carriers. Nature Reviews Drug Discovery. 2005;**4**:145-160. DOI: 10.1038/nrd1632

[32] Jeżowska I, Wolak A, Gruszecki WI, Strzałka K. Effect of β-carotene on structural and dynamic properties of model phosphatidylcholine membranes. II. A31P-NMR and 13C-NMR study. Biochimica et Biophysica Acta. 1994;**1194**:143-148. DOI: 10.1016/005-2736(94)90213-5

[33] Siegel DP. Inverted micellar intermediates and the transition between lamellar, cubic, and inverted hexagonal lipid phases. I. Mechanism of L_α H_{II} phase transitions. Biophysical Journal. 1986;**49**(6):1155-1170. DOI: 10.1016/S0006-3495(86)83744-4